Plant Physiology and Biochemistry 138 (2019) 65–79

Contents lists available at ScienceDirect

Plant Physiology and Biochemistry

journal homepage: www.elsevier.com/locate/plaphy

Research article

Formaldehyde assimilation through coordination of the glyoxylate pathway and the tricarboxylic acid cycle in broad bean roots

Yong Min, Wenjia Cao, Yun Xiong, Zhihao Si, Dawood Khan, Limei Chen*

Faculty of Life Science and Biotechnology, Kunming University of Science and Technology, Chenggong Campus, Chenggong, Kunming, 650500, China

ARTICLE INFO

Keywords:
Broad bean roots
HCHO assimilation
Glyoxylate pathway
TCA cycle
HCHO metabolic mechanism

ABSTRACT

Formaldehyde (HCHO) assimilation in broad bean (*Vicia faba* L. cv. YD) roots was investigated using ^{13}C-labeled HCHO followed by ^{13}C-NMR analysis. Results revealed that H^{13}CHO was first oxidized to H^{13}COOH in the roots treated with 2 mM H^{13}CHO in a time-dependent manner. Subsequently, a massive signal peak of [2, 4–^{13}C] citrate (Cit) and a signal peak of [2, 3–^{13}C]succinate (Su) were observed in accompany with an enhancement in the signal intensity of [3–^{13}C]Cit. The data suggested that the glyoxylate pathway and the tricarboxylic acid (TCA) cycle functioned simultaneously in the subsequent assimilation of H^{13}COOH. The yield of [2, 4–^{13}C]Cit accounted for more than 80% of the total metabolites. The activity of isocitrate lyase (ICL), a key enzyme in the glyoxylate pathway, was stimulated by HCHO in a dosage-dependent manner. As a result, [2, 4–^{13}C]Cit production was increased significantly in YD roots treated with high concentrations (4 and 6 mM) of H^{13}CHO. Moreover, induction of the ICL activity by methanol resulted in a simultaneous elevation in the production of [2, 4–^{13}C]Cit and [3–^{13}C]Cit in methanol-pretreated roots under 2 mM H^{13}CHO stress. Pretreatment of roots with cyclosporin A, which hinders the transport of ^{13}C-enriched compounds into mitochondria, caused a notable decline in the signal peak and yield of [2, 4–^{13}C]Cit and consequently induced a notable accumulation of [2, 3–^{13}C]Su and an increase in the HCO_3^- production (generated from H^{13}COOH oxidation) in H^{13}CHO-treated roots. These results suggested that the glyoxylate pathway and the TCA cycle function coordinately in HCHO assimilation in broad bean roots.

1. Introduction

Formaldehyde (HCHO) is used in many industrial syntheses and production processes, which results in the generation of a large amount of HCHO-containing wastewater (Xu et al., 2008). In addition, use of environment-unfriendly materials in decoration can also cause HCHO pollution in indoor air (Flyvholm and Andersen, 1993). The indoor-air HCHO pollution has become a major environmental problem in developing countries (Main and Hogan, 1983). HCHO is considered one of the most active and electrophilic chemical, which can bind non-specifically with a variety of lipids, nucleic acids and proteins. This binding often results in loss of biological activity of many macromolecules in various organisms (Feldman, 1973). As a result, exposure to HCHO may cause dysfunction of many tissues and organs in animals and human (Main and Hogan, 1983).

HCHO pollution has been related to extensive damages to human health, development of remediation technology for HCHO pollution has received significant attention. Among the remediation technologies for practical application, phytoremediation is considered to be environment-friendly and sustainable technology. Recent investigations have shown that, in the plant-purification system, leaves can absorb HCHO from the polluted air and convert it into carbohydrates and amino acids via the Calvin cycle and C1 metabolism (Kim et al., 2018). Roots can absorb HCHO in wastewater when HCHO-contaminated wastewater flows through a bioreactor consisting of plant roots and soil (Xu et al., 2010). Recent studies on the HCHO metabolic mechanisms have indicated that the HCHO absorbed by leaves can be assimilated to sugars, organic acids or amino acids, which then eventually integrated into cell components, such as celluloses, starches and proteins (Kim et al., 2018). The HCHO assimilation pathways show diversity in different plant species. For example, the assimilation pathway of HCHO conversion to methionine (Met) was observed only in the petunia leaves exposed to a low concentration of liquid HCHO (Zhang et al., 2014). When Petunia leaves were exposed to a high concentration of HCHO, the HCHO assimilation was shifted to a different pathway in which HCHO is initially oxidized to formate, and formate is condensed to glyoxylate. Afterwards it is assimilated to glycine (Gly) (Zhang et al., 2014; Sun et al., 2015). The assimilation pathway of HCHO conversion

* Corresponding author.
E-mail address: chenlimeikm@126.com (L. Chen).

https://doi.org/10.1016/j.plaphy.2019.02.019
Received 1 November 2018; Received in revised form 19 February 2019; Accepted 19 February 2019
Available online 26 February 2019

to citrate (Cit) was only observed in banana (Zeng et al., 2014) and geranium (Zhou et al., 2015) leaves treated with HCHO. In HCHO-treated *Arabidopsis thaliana* leaves, HCHO can be assimilated to Gly and serine (Ser) via photorespiration. Simultaneously, HCHO is also assimilated to nitrogen-transport amino acids through the tricarboxylate (TCA) cycle (Song et al., 2013). In HCHO-treated tobacco leaves, HCHO is assimilated to glutamine (Gln) and Asparagine (Asn) via the phosphoenolpyruvate carboxylase reaction and the TCA cycle (Wang et al., 2016).

The glyoxylate can be produced through the photorespiration pathway and the glyoxylate cycle in plants. In addition, it has been shown that formate can be condensed to glyoxylate by glyoxylate synthase (Arora et al., 1985) in the chloroplasts of green potato tubers. Glyoxylate plays an important role in the metabolism of amino acids in plants. The ^{14}C-labeled glyoxylate is rapidly metabolized in leaves, cotyledons and roots of many plants to produce organic acids, including glutamate (Glu), aspartate (Asp), Gly, Ser, Malate (Mal), Cit, Succinate (Su) and glycollate, CO_2 and a small amount of carbohydrates (Sinha and Cossins, 1965). Based on the data obtained from the C^{13}-NMR analysis of HCHO metabolic profiles in plants, we speculated that the glyoxylate pathway might play an important role during HCHO assimilation in plant tissues exposed to HCHO solutions. Most of the previous studies have focused on investigations of HCHO metabolism and assimilation in leaves, a photosynthetic organ of plants (Kim et al., 2018). Almost no studies on HCHO metabolism in roots (a non-photosynthetic organ) have been conducted. When rice plants experience hypoxia, such as flooding, expression of key enzymes, isocitrate lyase (ICL) and malate synthase (MS), in the glyoxylate pathway, is strongly induced (Lu et al., 2005). Consequently, the activity of ICL and MS is significantly increased, which in turn enhances the role of the glyoxylate pathway. Under hypoxia conditions, a large amount of acetaldehyde and acetate are produced in rice leaves due to enhanced glycolysis. Aldehyde and acetate can be detoxified by conversion to Cit and Mal via the enhanced glyoxylate pathway (Lu et al., 2005).

Our preliminary study showed that the roots of a broad bean cultivar (YD) could absorb HCHO. This study was intended to investigate the HCHO uptake kinetics and to reveal the HCHO metabolic mechanism in YD roots by ^{13}C-NMR analysis. By using some compounds that regulated the ICL activity, we investigated the role of the glyoxylate pathway in HCHO metabolism and assimilation in YD roots. The results verified that the glyoxylate pathway and the TCA cycle played an important role in HCHO assimilation in YD roots.

2. Materials and methods

2.1. Cultivation of YD plants

Seeds of YD (*Vicia faba* L. cv. YD) were obtained from the Yunnan Academy of Agricultural Sciences (Kunming, Yunnan Province, China). YD plants were grown under greenhouse conditions as previously described (Chen et al., 2013). After growing for 2–3 weeks, YD plants were used for the following experiments.

2.2. HCHO treatments and HCHO uptake measurements

Roots (3 g fresh weight, FW) were collected from YD plants and treated in 150 ml of HCHO solution [containing 5 mM $KHCO_3$, 0.1% MES (2-(N-morpholino)-ethanesulfonic acid (w/v) and 2, 4, or 6 mM HCHO] in a plant tissue culture bottle. The treatment was carried out at 25 °C under continuous light (100 μmol m^{-2} s^{-1}) conditions. The concentration of the residual HCHO in the treatment solutions was measured at indicated time points with the Nash reagent (consisting of 2 M ammonium acetate, 50 mM acetic acid and 20 mM acetylacetone) as described by Nash (1953). The same treatment solutions without roots incubated under the same conditions served as controls for monitoring the volatilization of HCHO. Dead roots (killed by heating at 95 °C for 5 min) were treated in the same way and used to measure the adsorbed HCHO. Three replicates were set up for each treatment. The adsorbed HCHO by dead roots was calculated as 100% (the initial level) - residual HCHO% in treatment solutions with dead roots - volatilized HCHO%. The absorbed HCHO by living roots was calculated as 100% (the initial level) - residual HCHO% in treatment solutions with living roots - volatilized HCHO% - HCHO% adsorbed by dead roots. After treatment, roots were washed with sterile water for 2–3 times and extra moisture was blotted using filter paper. The roots were then frozen in liquid nitrogen and stored at −80 °C for enzyme activity analysis.

2.3. ICL enzyme activity assays

Based on the data documented in the reference (Ismail et al., 1997), glucose, mannose and sucrose can inhibit the expression of ICL (EC 4.1.3.1), a key enzyme in the glyoxylate pathway. In this study, YD roots were treated with 5, 15, and 25 mM of glucose, mannose and sucrose for 2 h. Changes in the ICL activity in YD roots were analyzed to verify if these sugars have a significant inhibitory effects on ICL activity in YD roots. Moreover, our recent study showed that application of methanol in black soybean roots induces the expression of genes encoding HCHO metabolism-related enzymes (Tan et al., 2017). Therefore, methanol at the concentrations of 2, 4, 6 and 10 mM was used to treat YD roots for 2 h.

For ICL activity assay, proteins were extracted as described by Maxwell et al. (1975). The protein extraction buffer consisted of 50 mM potassium-phosphate buffer (pH 7.5), 5 mM $MgCl_2$, 0.4 mM EDTA, 1.5 mM dithiothreitol and 2% (w/v) glycerol. The frozen roots (1 g FW) were ground in 3 ml of extraction buffer in a precooled mortar with a pestle. The homogenate was centrifuged at 12,000 × *g* at 4 °C for 20 min and the supernatant was collected. Protein concentration in the supernatant was measured using a Bio-Rad protein assay kit with bovine serum albumin (BSA) as the standard. The extract with 100 μg protein was used for the enzyme activity assay. ICL activity was determined based on the amount of generated glyoxylate phenylhydrazone by measuring the absorbance at 324 nm at 25 °C (Cooper and Beevers, 1969). One unit of enzyme activity equals to the formation of 1 nmol of glyoxylate phenylhydrazone min^{-1}.

2.4. H^{13}CHO labeling experiments

H^{13}CHO was purchased from Cambridge Isotopes Laboratories (Andover, MA). In the time course labeling experiments, freshly excised YD roots (3 g FW) were treated with 100 ml of an H^{13}CHO solution containing 5 mM $KHCO_3$ and 0.1% MES (w/v) for 0.5, 2, 4, 12, 24 and 48 h. In the concentration labeling experiments, YD roots were treated with 2, 4 or 6 mM H^{13}CHO for 2 h. The labeling experiments were carried out under constant light (100 μmol m^{-2} s^{-1}) conditions at 25 °C.

Based on the above experimental results, YD roots were pretreated with 10 mM methanol for 2 h following by a treatment with 2 mM H^{13}CHO for 8 h to analyze the effect of methanol on the H^{13}CHO assimilation in YD roots.

Cyclosporine (CSA) is a specific inhibitor for mitochondrial permeability transport pores in animal cells. To investigate the role of the mitochondria-localized TCA cycle in HCHO assimilation, YD roots were pretreated with 25 μM CSA for 6 h according to the method described by Song et al. (2013), followed by a treatment with 2 mM H^{13}CHO for 24 h.

After H^{13}CHO labeling, roots were washed with cooled sterile water for 5 times to remove free H^{13}CHO from the root surfaces and extra water on root surfaces was blotted using filter papers. The roots were immediately frozen in liquid nitrogen and stored at −80 °C for extraction of metabolites.

2.5. Extraction of metabolites and ^{13}C-NMR analysis

Frozen roots were ground to fine powder with a pestle mortar and extracted with 4 ml of 100 mM potassium phosphate buffer (KPB, pH 7.4). After thawing, the extract was boiled for 3 min and centrifuged at 12,000 rpm for 10 min to remove cellular debris. The supernatant was frozen, lyophilized and re-suspended in 0.5 ml of 100 mM KPB containing 5% (v/v) D_2O. Then, the extract was transferred to a 5-mm NMR tube ^{13}C-NMR analysis.

The ^{13}C-NMR analysis was performed on a Bruker DRX 500-MHz instrument (Bruker Biosciences Corporation, Billerica, MA, USA). ^{13}C-NMR data were collected according to previously described parameters (Chen et al., 2010). The acquisition parameters include a 5-μs (90°) pulse with broadband proton decoupling, a spectral width of 37,594 Hz, an acquisition time of 0.5 s, and a decay time of 1.2 s. The sample temperature was maintained at 25 °C, and 32,000 data points were acquired for each sample. Twelve hundred scans were acquired for each sample, and a line broadening of 4 Hz was used to process the data.

In the ^{13}C-NMR spectra, chemical shifts were referenced to methanamide resonance (Ref) at 166.85 ppm. ^{13}C-NMR spectra were calibrated to the reference for comparison of interested peaks in different samples. Resonance peaks were assigned by comparisons with authentic compound, chemical shifts and confirmed by spiking the KPB extracts with authentic reference standards. To compare the relative contents of metabolites, target peaks were integrated to the reference (set as 1).

2.6. Statistical analysis

Three replicates were conducted for all analyses. Statistical analysis was carried out using the analytical software Statistical Product and Service Solutions (SPSS 11.5). Means were separated by analysis of variance (ANOVA) and significant differences were assessed by Duncan's multiple range test at $P < 0.05$. The values represent the mean ± SD (n = 3). Different letters indicate significant differences at $P < 0.05$; the same letters indicate no significant differences at $P < 0.05$.

3. Results

3.1. The kinetics of HCHO uptake by YD roots from HCHO solution

To investigate the uptake kinetics of HCHO by YD roots from HCHO solutions, the detached YD roots were treated with 2, 4, or 6 mM HCHO solutions. The amount of residual HCHO (Fig. 1a), volatilized HCHO (Fig. 1b) and adsorbed HCHO (the uptake of HCHO by dead roots) (Fig. 1c) was measured at 0, 0.5, 2, 4, 12, 24 and 48 h. The results showed that the difference in the residual HCHO among the three treatment solutions with different concentrations was not significant in the entire treatment period. At the first 4-h treatment stage of the three treatment solutions, the decreases in the residual HCHO was slow (Fig. 1a), which indicates low efficiency of HCHO uptake by YD roots at this stage. When the treatment reached to the late stage (12–48 h), the residual HCHO in the three treatment solutions was sharply declined (Fig. 1a), suggesting that the efficiency of HCHO uptake was notably increased. The volatilized HCHO from the 2, 4, and 6 mM HCHO solutions during the entire treatment period accounted for ~3%, ~4% and 5%, respectively, of the initial HCHO in the treatment solutions (Fig. 1b). During the entire treatment period, the dead YD roots adsorbed ~3%, ~3.5% and ~4% HCHO from the 2, 4 and 6 mM treatment solutions, respectively (Fig. 1c). The data suggest that the HCHO adsorbed by the dead roots had only a small contribution to the HCHO removal.

The uptake of HCHO by living roots from the treatment solution were calculated based on the residual HCHO, the volatilized HCHO and adsorbed HCHO by dead roots to construct the HCHO uptake curves (Fig. 1d). According to the HCHO uptake curves, the correlation between the HCHO uptake (y) and time (x) during the entire treatment period (0–48 h) was in line with an exponential function ($y = e^x$). At the early treatment stage (0–4 h), only small amounts of HCHO were absorbed by YD roots from the treatment solutions, accounting for ~20% of the initial HCHO in each of the three treatment solutions. During the period of 4–24 h, HCHO uptake by living YD roots was markedly increased, resulting in a notable decline in the residual HCHO in the treatment solutions. More than 90% HCHO was absorbed by living YD roots from each solution after treatment for 48 h. The increase in the uptake of HCHO at the late stage might be associated with the enhanced HCHO metabolism in living roots.

3.2. Coordinated functions of the glyoxylate pathway and TCA cycle during $H^{13}CHO$ assimilation in YD roots treated in the low-level $H^{13}CHO$

To decipher the HCHO metabolic pathway in YD roots, the detached roots were treated with 2 mM $H^{13}CHO$ and the $H^{13}CHO$ metabolites were analyzed using ^{13}C-NMR (Supplementary Fig. S1). The relative content of the main metabolites was estimated based on the integration of respective signal peaks relative to that of the reference (Ref). The ^{13}C-NMR spectra of $H^{13}CHO$-treated YD roots at different treatment stages were compared with the ^{13}C-NMR spectra of the control roots (CK). The signal peak of $H^{13}COOH$ (FA) appeared in the 0.5-h spectrum (Fig. 2a and c), indicating quick production of $H^{13}COOH$ during $H^{13}CHO$ metabolism in YD roots. The intensity of the $H^{13}COOH$ signal peak was elevated with the increased treatment time from 0.5 h to 12 h (Fig. 2a and c), suggesting that the yield of $H^{13}COOH$ was increased with the treatment time during the period of 0.5–12 h. However, the $H^{13}COOH$ signal was almost undetectable in the 24-h and 48-h spectra (Fig. 2a, b and 2c), indicating the complete conversion of $H^{13}COOH$ to other metabolites. A clear CO_2 signal peak in the form of HCO_3^- was detected in the 12-h spectrum (Fig. 2a). This signal peak was elevated at 24 h and became stronger in the 48-h spectrum (Fig. 2a and d). The data indicate the formation of CO_2 during the $H^{13}CHO$ metabolism in YD roots over the period of 12–48 h. The signal peak of [2,3–^{13}C]succinate (Su) appeared in the 24-h spectrum and was obviously enhanced in the 48-h spectrum (Fig. 2b). The signal intensity of this peak was increased by ~14-fold at 48 h compared to that of 24 h (Fig. 2e), indicating that a large amount of [2,3–^{13}C]Su was produced in YD roots with 2 mM $H^{13}CHO$ treatment for 48 h.

The presence of strong signal peaks of [1,3,5–^{13}C]Cit in the control (CK) spectrum suggests that Cit is an abundant organic acid in YD roots (Fig. 2f). The signal peak of [3–^{13}C]Cit was elevated significantly at 0.5 h (Fig. 2f) and maintained at the similar intensity during the period of 2–48 h (Fig. 2g). Moreover, a major signal peak of [2,4–^{13}C]Cit appeared in the 0.5-h spectrum (Fig. 2f). This signal peak reached the highest level at 2 h (Fig. 2f), with the signal intensity almost ~3-fold that at 0.5 h (Fig. 2h). The signal intensity of this peak maintained at the similar level during the 4–24 h period (Fig. 2h). The results suggest that a large amount of [2,4–^{13}C]Cit was generated during $H^{13}CHO$ metabolism in YD roots exposed to 2 mM $H^{13}CHO$. During the period of 24–48 h, the signal intensity of [2,4–^{13}C]Cit peak declined significantly (Fig. 2h). The [6–^{13}C]Cit signal peak was absent in CK but was observed in the 48-h spectrum (Fig. 2f), suggesting the production of [6–^{13}C]Cit at 48 h. The evidence from the ^{13}C-NMR analysis indicates that the ^{13}C signal was selectively enriched in different carbons of Cit during $H^{13}CHO$ metabolism in YD roots.

Since the signal peaks of [2,4–^{13}C]Asn (Fig. 2k) and [1,3,5–^{13}C]Glu (Fig. 2n) are strong in the CK spectrum, these two compounds are the abundant amino acids in YD roots. The signal peaks of [2,4–^{13}C]Asn and [3,5–^{13}C]Glu was enhanced at 0.5 h (Fig. 2k and n) and remained at the similar intensity from 4 h to 24 h (Fig. 2l, m, o and q). Furthermore, a strong signal peak of [2–^{13}C]Asp was detected at 48 h (Fig. 2j). The signal peak of [4–^{13}C]Glu appeared at 0.5 h (Fig. 2n), elevated at 2 h (Fig. 2n) and reached to its highest level at 4 h (Fig. 2p). However, the signal intensity of this peak showed a decreasing trend from 12 h to

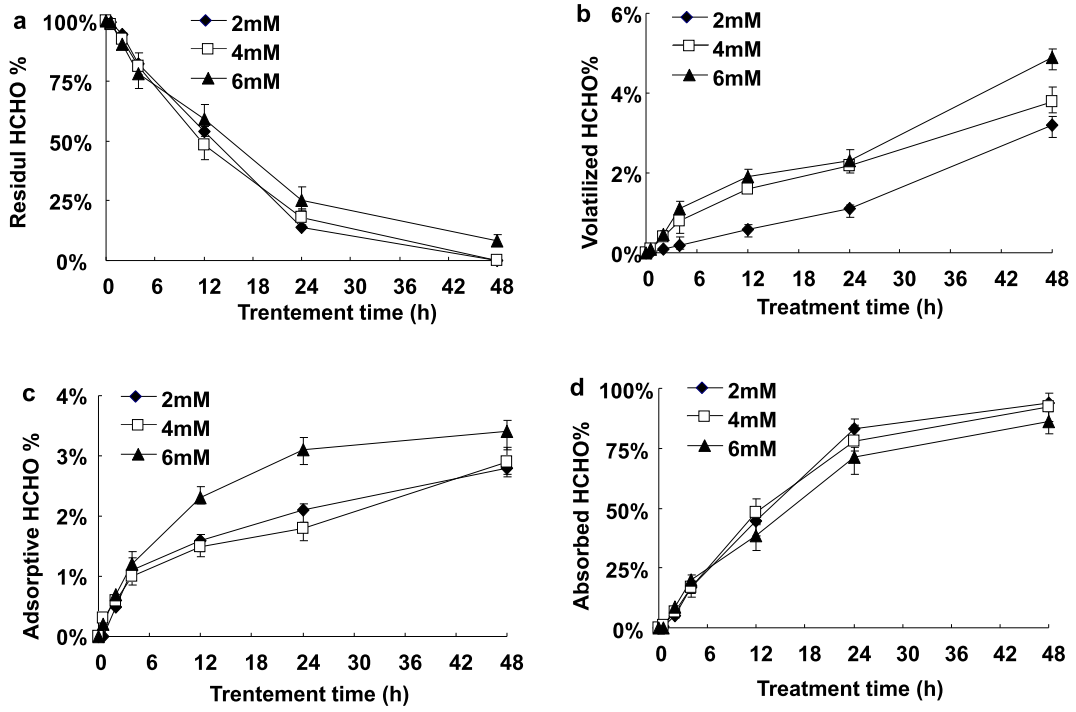

Fig. 1. The HCHO uptake kinetics of broad bean (YD) roots treated with 2, 4 or 6 mM HCHO solutions. (a) Residual HCHO in 2, 4 or 6 mM HCHO solutions after living roots were treated for 0.5–48 h. (b) Volatilized HCHO from 2, 4 and 6 mM solutions. (c) Adsorbed HCHO by dead roots from 2, 4 and 6 mM solutions. The adsorbed HCHO were obtained by using the initial HCHO to subtract the residual HCHO in treatment solutions with dead roots and volatilized HCHO. (d) HCHO uptake curves. The HCHO uptake curves were produced by using the initial HCHO to subtract the residual HCHO in treatment solutions with living roots, volatilized HCHO and adsorbed HCHO by dead roots.

48 h (Fig. 2p). Based on these data, we concluded that a considerable amount of Asn, Glu and Asp were produced during the period of 4–48 h in YD roots with 2 mM $H^{13}CHO$ treatment.

In addition, the [2–^{13}C]Gly peak appeared in the 0.5-h spectrum and was sharply elevated to the highest level at 2 h (Fig. 2r). However, the signal intensity of this peak started to decline at 4 h (Fig. 2t), rapidly decreased at 12 and 24 h and disappeared at 48 h after the $H^{13}CHO$ treatment (Fig. 2r and t). These results suggest that the $H^{13}CHO$ metabolism produces a considerable amount of [2–^{13}C]Gly in YD roots during early stages (0.5–4 h) yet this metabolite is likely converted to other compounds later (12–24 h). The signal peak of [3–^{13}C]Ser was enhanced significantly at 4 h and continuously elevated in the 12-h spectrum (Fig. 2s). However, the signal intensity of this peak was reduced significantly in the period of 24–48 h (Fig. 2s and u). This result indicates that a certain amount of [3–^{13}C]Ser was generated during the period of 12–24 h. A strong peak of [3–^{13}C]cysteine (Cys) was observed in the CK sample (Fig. 2s), suggesting a relatively high content of Cys in YD roots (Fig. 2v). This signal peak was decreased rapidly after 2 mM $H^{13}CHO$ treatment and was not elevated during the entire treatment period (Fig. 2s and v). The result indicates no production of Cys in 2 mM $H^{13}CHO$-treated YD roots.

The presence of [U−^{13}C] glucose (Gluc) and [U−^{13}C] fructose (Fruc) peaks in the CK spectrum (Fig. 2w) indicates that there are abundant free Gluc and Fruc in YD roots. Comparison between the spectra of 2 mM $H^{13}CHO$-treated samples and the CK revealed a gradual decrease in the intensity of [U−^{13}C]Gluc (Fig. 2x) and [U−^{13}C]Fruc (Fig. 2y) peaks during the treatment period. The result suggest that HCHO treatment caused consumption of endogenous sugars, which might be ascribe to aggravate glycolysis in YD roots under HCHO stress. The signal peaks of [U−^{13}C] Gluc and [U−^{13}C] Fruc were not recovered until 48 h after 2 mM $H^{13}CHO$ treatment (Fig. 2w). The evidence implies that these sugars were not generated from the $H^{13}CHO$ metabolism in YD roots.

Gly, Ser and CO_2 were shown to be major metabolites in [2–^{14}C] glyoxylate-treated plant tissues such as storage organs, leaves, cotyledons, coleoptiles and roots (Sinha and Cossins, 1965). Moreover, a considerable amount of ^{14}C-incorporation appeared in amino acids and organic acids, such as Glu, Asp, Mal, Cit, and Su. These organic acids and amino acids are the major products of glyoxylate metabolism in roots. $H^{13}CHO$ metabolism in 2 mM $H^{13}CHO$-treated YD roots produced Cit, Gly, Ser, Su, Asp, Glu, Asn and CO_2. The metabolite types for $H^{13}CHO$ metabolism in YD roots is similar to that of [2–^{14}C] glyoxylate metabolism in plant tissues, especially in root tissues. Furthermore, Cit and Gly was produced along with the formation of $H^{13}COOH$ in $H^{13}CHO$-treated YD roots. Accordingly, we proposed that $H^{13}CHO$ metabolism in YD roots might produce [^{13}C] glyoxylate, which was subsequently metabolized to produce Cit, Gly, Ser, Su, Asp, Glu and Asn.

The signal peak of [3–^{13}C] Cit started to increase at 0.5 h in YD roots after exposed to 2 mM $H^{13}CHO$. Based on this observation, we speculated that $H^{13}COOH$, produced from oxidation of $H^{13}CHO$, was condensed to ^{13}C-glyoxylate, which might enter the glyoxylate pathway. The ^{13}C label from ^{13}C-glyoxylate reached the 3-hydroxy carbon of Cit, thereby enhancing the [3–^{13}C] Cit signal peak. [2, 4–^{13}C]Cit is the most important product of $H^{13}CHO$ metabolism in 2 mM $H^{13}CHO$-treated YD roots. However, the ^{13}C label from ^{13}C-glyoxylate is not able to be designated to C2 and C4 of Cit through the glyoxylate pathway. Cit is a common metabolite between the glyoxylate pathway and TCA cycle. Thus, the pathway for the production of [2, 4–^{13}C] Cit in 2 mM $H^{13}CHO$-treated YD roots can be proposed as follows. The metabolism of [^{13}C] glyoxylate in the glyoxylate pathway produced [3, 6–^{13}C] Cit, which was isomerized to [2, 6–^{13}C]Icit. This metabolite was then cleaved to produce [2–^{13}C] Su. Further metabolism of [2–^{13}C] Su via the TCA cycle produced [2, 4–^{13}C] Cit. The observation of [6–^{13}C] Cit and [2, 3–^{13}C] Su signal peaks at 48 h validated the feasibility of this insight. Therefore, it is reasonable to conclude that both the glyoxylate pathway and the TCA cycle played synergetic roles during $H^{13}CHO$ assimilation in YD roots. Metabolism of [2, 4–^{13}C]Cit in the TCA cycle

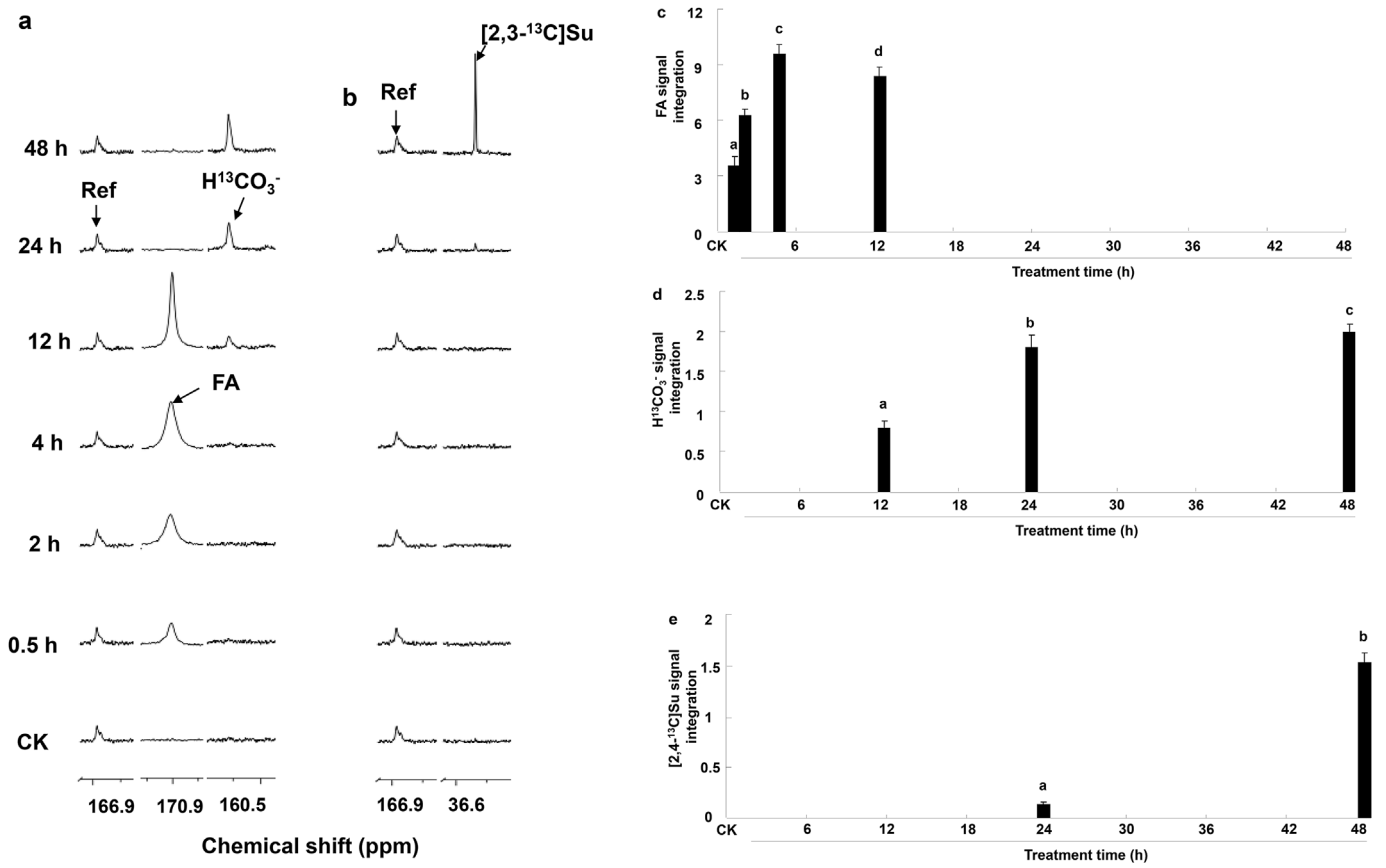

Fig. 2. Time course ^{13}C NMR spectra of YD roots treated with 2 mM H^{13}CHO for 0.5–48 h. The peak assignments are described as in Supplementary Fig. S1. The expanded regions of the signal peaks corresponding to $H^{13}CO_3^-$, HCOOH (FA), [2,3–^{13}C]Su, [6–^{13}C]Cit, [1,5–^{13}C]Cit, [3–^{13}C]Cit, [2,4–^{13}C]Cit, [2–^{13}C]Asp, [4–^{13}C]Asn, [2–^{13}C]Asn, [1–^{13}C]Glu, [3–^{13}C]Glu, [4–^{13}C]Glu, [5–^{13}C]Glu, [2–^{13}C]Gly, [3–^{13}C]Ser, [2–^{13}C]Cys, [U−^{13}C]Gluc and [U−^{13}C]Fruc) are shown in (a), (b), (f), (j), (k), (n),(r),(s) and (w). The signal integration of these peaks is shown in (c), (d), (e), (g), (h), (i), (l), (m), (o), (p), (q), (t), (u), (v), (x) and (y).

produced [3–^{13}C]α-ketoglutarate (KGA) and [2, 3–^{13}C] oxalacetate (OAA). Transamination of [3–^{13}C] KGA and [2, 3–^{13}C] OAA produced [3–^{13}C] Glu and [2–^{13}C]Asp. [2–^{13}C] Asp could be converted to [2–^{13}C] Asn by asparagine synthase. [2–^{13}C] Gly might be generated via transamination of ^{13}C-glyoxylate. Generation of CO_2 might be originated from two pathways: decarboxylation of [2–^{13}C] Gly or oxidation of H^{13}COOH. Decarboxylation of [2–^{13}C] Gly could produce 5,10-$^{13}CH_2$-THF, which reacted with the endogenous Gly to produce [3–^{13}C] Ser.

3.3. The role of the glyoxylate pathway and TCA cycle was enhanced in YD roots after exposed to high-concentration H^{13}CHO

To determine the roles of the glyoxylate pathway and TCA cycle in H^{13}CHO assimilation in the YD roots exposed to high concentration of H^{13}CHO, YD roots were treated with 4 and 6 mM H^{13}CHO for 2 h. The metabolic spectra of 4 and 6 mM H^{13}CHO-treated roots were compared with that of roots exposed to 2 mM H^{13}CHO (Supplementary Fig. S2). The results indicate that the metabolite spectra of YD roots treated with 4 mM and 6 mM H^{13}CHO are very similar to that of YD roots exposed to 2 mM H^{13}CHO. Production of H^{13}COOH (Fig. 3a and b) in YD roots was decreased while the generation of CO_2 (Fig. 3a and c) became notable with the elevation of H^{13}CHO concentrations. Moreover, the signal peaks of [2, 4–^{13}C]Cit (Fig. 3d and e) and [4–^{13}C] Glu (Fig. 3f and g) were increased significantly (10.4%) in 4 and 6 mM H^{13}CHO-treated roots. Results indicated that more [2, 4–^{13}C]Cit was produced in YD roots exposed to high-concentration of H^{13}CHO solutions, implying an enhancement in the role of the glyoxylate pathway and TCA cycle during H^{13}CHO assimilation. The signal peak of [2–^{13}C] Gly showed similar intensity in 2 and 4 mM H^{13}CHO-treated roots (Fig. 3h and i). However, a notable decline was observed in this signal peak in 6 mM H^{13}CHO-treated roots (Fig. 3h and i), indicating a reduced generation of [2–^{13}C]Gly. Compared to those in 2 mM H^{13}CHO-treated roots, the signal intensities of [3–^{13}C]Cys (Fig. 3h and j), [U−^{13}C]Gluc (Fig. 3k and l) and [U−^{13}C]Fruc peaks (Fig. 3k and m) were all declined in 4 and 6 mM H^{13}CHO-treated roots. The data suggest that treatment with 4 and 6 mM H^{13}CHO did not induce the generation of sugars and Cys in YD roots during H^{13}CHO metabolism.

3.4. HCHO and methanol induced the activity of ICL in YD roots

ICL is one of the key enzymes in the glyoxylate pathway, which catalyzes the cleavage of Icit to Su and glyoxylate. Su is the key metabolite that connects the glyoxylate pathway and the TCA cycle. The main metabolite, [2, 4–^{13}C]Cit, was produced by the combined functions of the glyoxylate pathway and the TCA cycle during H^{13}CHO metabolism in YD roots. The production of [2,4–^{13}C]Cit was increased with the increase in 2 mM H^{13}CHO treatment time as well as the H^{13}CHO concentration during a short treatment period (2 h). Therefore, we investigated the effect of HCHO on the ICL activity in YD roots. Results showed that the changing pattern of the ICL activity was consistent with that of [2, 4–^{13}C]Cit signal intensity under 2 mM HCHO treatment (Fig. 4a). The ICL activity in YD roots was significantly elevated after 2 mM HCHO treatment for 2 h (Fig. 4a), indicating that HCHO has a significant induction on the ICL activity in YD roots. The ICL activity reached its maximal level at 2 h (Fig. 4a), and the [2, 4–^{13}C]Cit production also reached its highest yield in YD roots exposed to 2 mM H^{13}CHO for 2 h. The ICL activity in YD roots decreased after

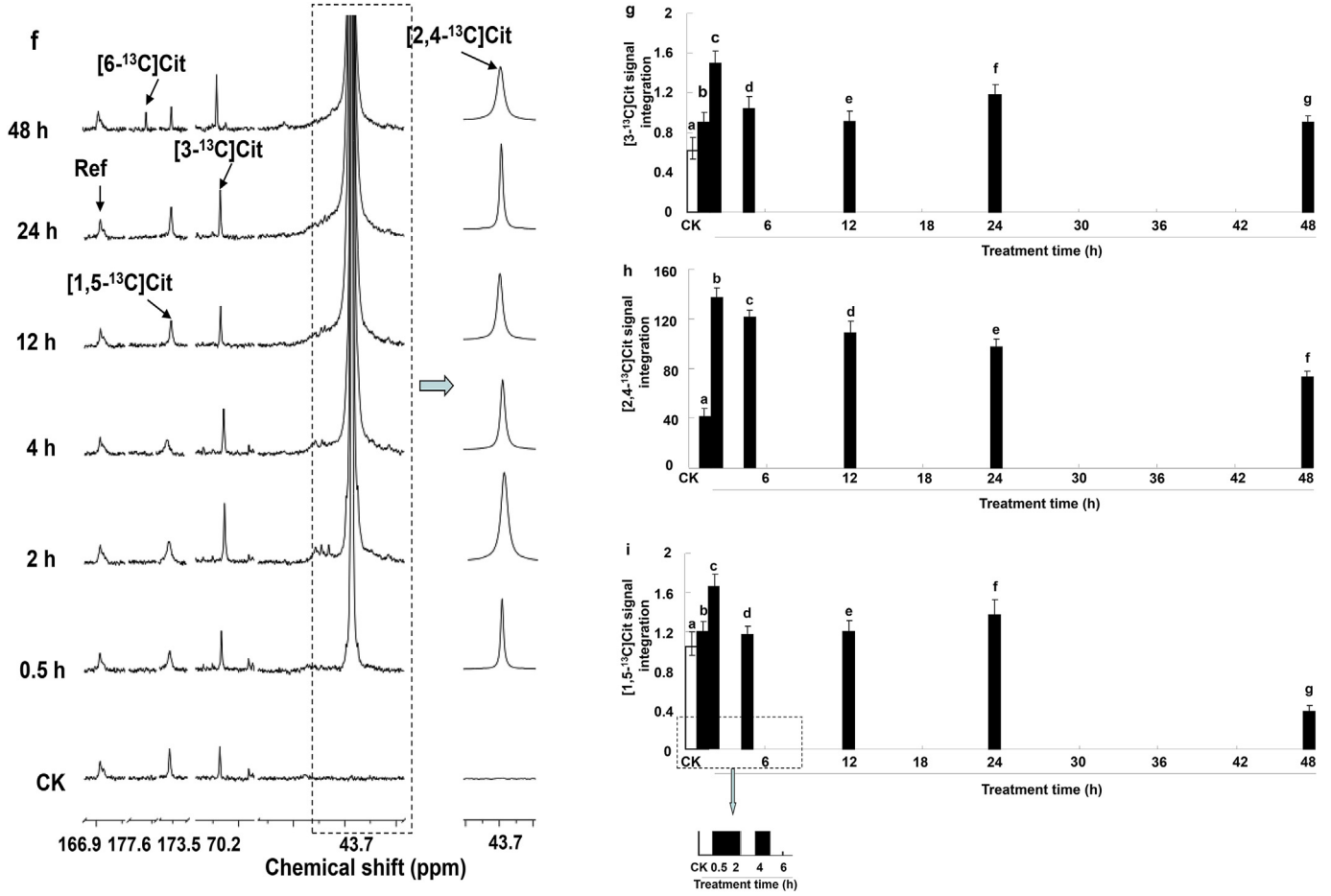

Fig. 2. (*continued*)

2 mM HCHO treatment for 12 h (Fig. 4a). At this point, the production of [2, 4–^{13}C]Cit was also decreased significantly. The ICL activity in YD roots was further declined when the treatment was extended to 24 h (Fig. 4a). Similarly, the decrease in [2, 4–^{13}C] Cit production also became much more pronounced at 24 h.

The changing pattern of ICL activity under high concentration (4 mM and 6 mM) of HCHO treatments (Fig. 4b) was also consistent with that of [2,4–^{13}C]Cit production in YD roots. The ICL activity in 4 and 6 mM HCHO-treated YD roots was higher than that in 2 mM HCHO-treated roots (Fig. 4b). These results demonstrated that the induction of ICL activity by 4 mM and 6 mM HCHO was greater than that by 2 mM HCHO, which may explain why the [2,4–^{13}C]Cit production in 4 mM and 6 mM H^{13}CHO-treated roots was greater than that in 2 mM mM H^{13}CHO-treated roots.

A previous study has shown that the expression of *ICL* and *MS* genes in the glyoxylate pathway is regulated by endogenous sucrose, glucose, and fructose in cucumver cultured cells (Graham et al., 1994). The presence of glucose analogs, such as 2-deoxyglucose and mannose, specifically inhibit the expression of *ICL* and *MS* in cucumber cultured cells (Graham et al., 1994). Supplementation of sucrose inhibits the expression of *ICL* and *MS* in cucumber detached roots or hair roots (Ismail et al., 1997). We measured the ICL activity in YD roots treated with sucrose, glucose and mannose at 5, 15 and 25 mM (Fig. 4c). The results showed that 5 mM sucrose and mannose had slight induction yet 5 mM glucose had no significant effects on the ICL activity in YD roots (Fig. 4c). Treatments with sucrose, glucose and mannose at 15 and 25 mM for 2 h had no inhibition on the ICL activity in YD roots (Fig. 4c), indicating that the ICL activity in YD roots might not be regulated by these sugars.

Our recent studies have shown that methanol induces the expression of genes involved in the HCHO metabolism in black soybean roots. Therefore, in this study, the activity of ICL in YD roots treated with 2, 4, 6 and10 mM methanol for 2 h was determined (Fig. 4d). The results showed that methanol at high concentrations (6 and 10 mM) but not at low concentrations (2 and 4 mM) had a significant induction on the ICL activity in YD roots (Fig. 4d). Treatment with 6 mM methanol for 2 h led to a ~27% increase in the ICL activity (Fig. 4d). Treatment with 10 mM methanol increased the ICL activity by ~66.7% in YD roots (Fig. 4d). As a result, methanol was used as an activator for the ICL activity in subsequent experiments.

3.5. Methanol pretreatment enhanced the roles of the glyoxylate pathway and the TCA cycle during HCHO assimilation in YD roots

Based on the above results, YD roots were pretreated with 10 mM methanol for 2 h to induce the ICL expression followed by treatment with 2 mM H^{13}CHO for 24 h. The ^{13}C-NMR analysis was performed to detect the H^{13}CHO metabolites in YD roots. The metabolic profile of the methanol-pretreated roots was compared with that of the roots without methanol-pretreatment (Supplementary Fig. S3). Results showed that 10 mM methanol pretreatment led to an increase in H^{13}COOH production (Fig. 5a and b) but a decrease in CO_2 production (Fig. 5a and c) in H^{13}CHO metabolism. Methanol pretreatment significantly enhanced the signal peaks of [2, 4–^{13}C]Cit and [3–^{13}C]Cit (Fig. 5d). Consequently, the signal intensity of [2, 4–^{13}C] Cit was increased by 40% (Fig. 5e) and the [3–^{13}C]Cit signal peak was increased by 2.4-fold (Fig. 5f). Simultaneously, the production of [3–^{13}C]Glu (Fig. 5g and h) and [4–^{13}C]Glu (Fig. 5g and i) was increased by 57% and 50%, respectively. Production of these metabolites requires combined function of the glyoxylate pathway and the TCA cycle. The results suggest that

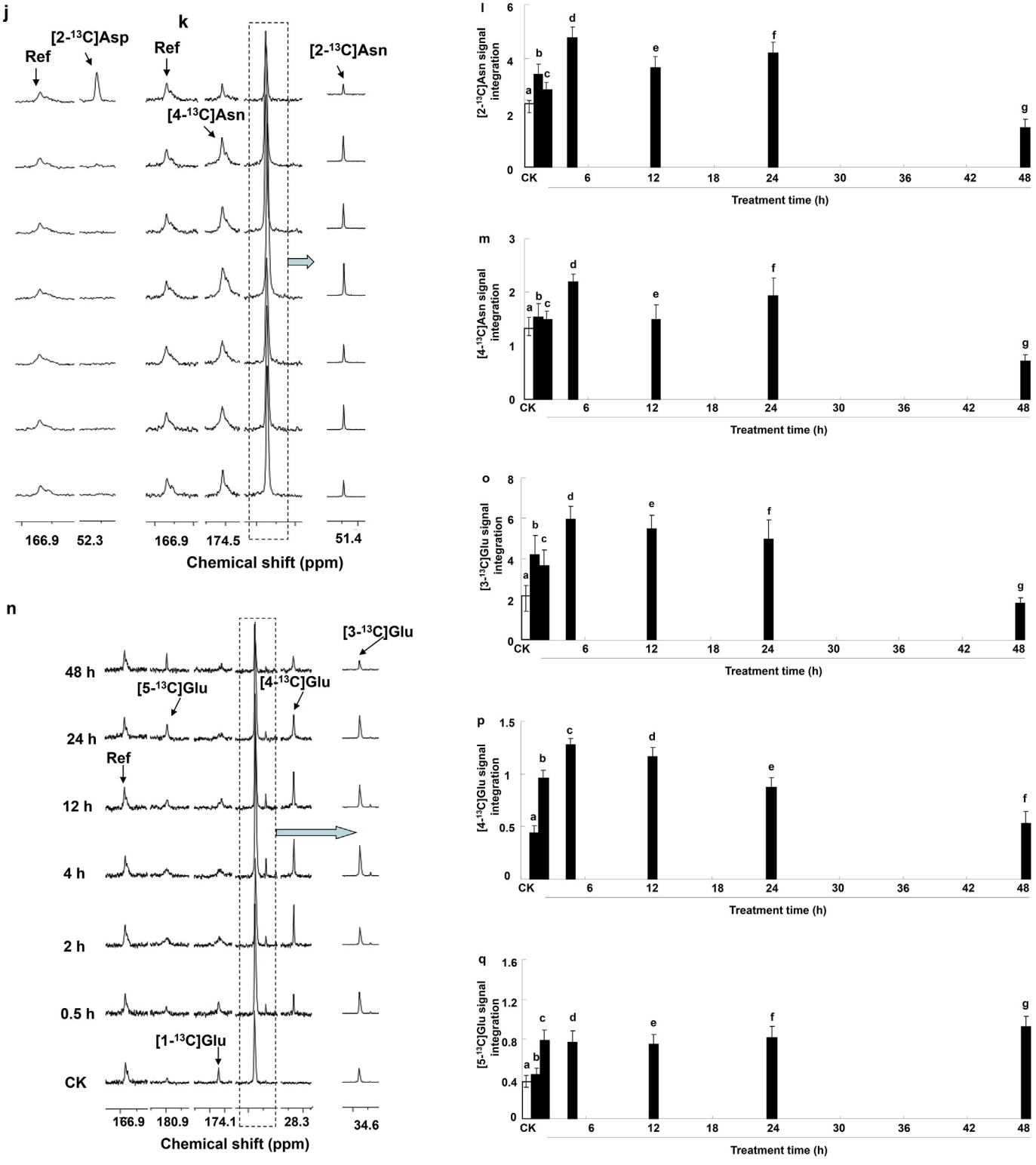

Fig. 2. (*continued*)

using of methanol as an inducer to increase the ICL activity could enhance the function of the glyoxylate pathway and the TCA cycle during HCHO assimilation.

3.6. Inhibition of mitochondrial permeability transition pores suppressed the roles of the glyoxylate pathway and TCA cycle during $H^{13}CHO$ assimilation in YD roots

Previous studies have shown that CSA, a specific inhibitor of mitochondrial permeability transition pores (MPTPs) in animal cells, inhibited the function of the HCHO metabolic pathway associated with mitochondria in Arabidopsis (Song et al., 2013), tobacco (Wang et al.,

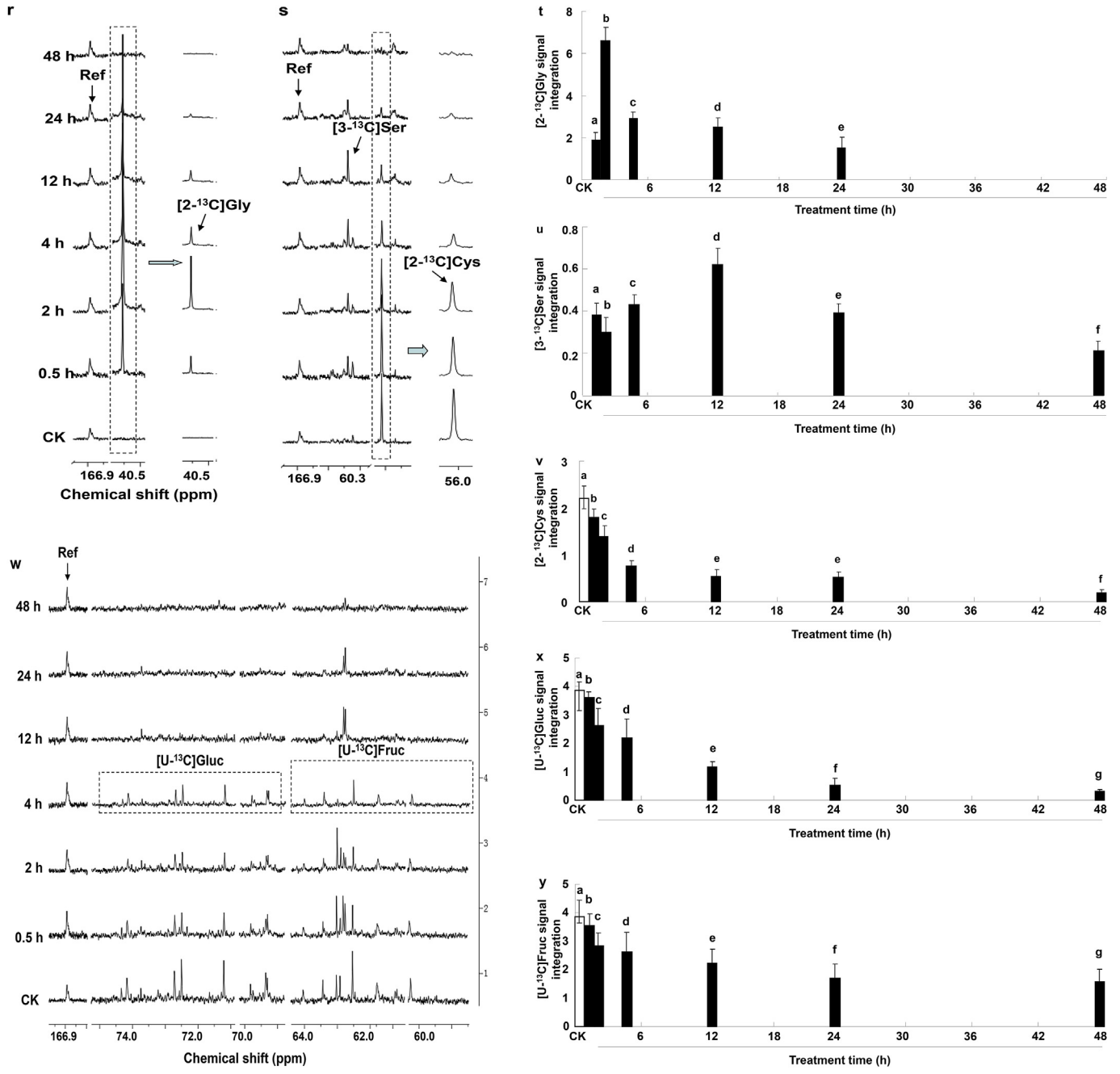

Fig. 2. (*continued*)

2016) and petunia (Zhang et al., 2014) leaves. To confirm the role of the TCA cycle in HCHO assimilation, YD roots was pretreated with 25 μM CSA for 2 h followed by a treatment with 2 mM $H^{13}CHO$ for 24 h. The ^{13}C-NMR analysis was performed to detect the ^{13}C-labeled metabolites in YD roots. The 24-h $H^{13}CHO$ metabolic profile of YD roots with CSA pretreatment was compared with that of roots without CSA pretreatment (Supplementary Fig. S4). Results revealed that signal peaks of [2, 4–^{13}C] Cit (Fig. 6a), [3, 4–^{13}C] Glu (Fig. 6c) and [2–^{13}C] Asn (Fig. 6f) were notably decreased in YD roots pretreated with CSA.

CSA pretreatment caused a 20%, 35–40% and 50% decrease in the production of [2, 4–^{13}C] Cit (Fig. 6b), [3, 4–^{13}C] Glu (Fig. 6d and e) and [2–^{13}C]Asn (Fig. 6g), respectively. These results could be attributed to the CSA-inhibited generation of [2, 4–^{13}C]Cit, [3, 4–^{13}C]Glu, [2–^{13}C]Asn in YD roots through the TCA cycle, which functions in the mitochondria. Moreover, the signal peaks (Fig. 6f and i) and yields (Fig. 6h and j) of [2–^{13}C]Gly and [3–^{13}C]Ser were also greatly reduced in CSA-pretreated roots. The data implied that the generation of [2–^{13}C]Gly and [3–^{13}C]Ser in YD roots during $H^{13}CHO$ metabolism were all inhibited due to the CSA pretreatment. If the generation of [2–^{13}C]Gly was located in peroxisome, it is plausible that CSA pretreatment hindered the generation of [2–^{13}C]Gly. The decarboxylation of [2–^{13}C]Gly, which provides the 5,10-$^{13}CH_2$-THF for the synthesis of [3–^{13}C]Ser, also occurs in the mitochondria. Thus, CSA pretreatment could inhibit the production of [3–^{13}C]Ser from $H^{13}CHO$ metabolism in YD roots. The evidence confirmed that the TCA cycle had a critical role in $H^{13}CHO$ assimilation in YD roots.

The signal peak of HCO_3^- was strongly enhanced (Fig. 6k) and the yield of HCO_3^- increased by 1-fold (Fig. 6l) in CSA-pretreated roots. The data suggest that the generation of CO_2 was originated from the oxidation of FA rather than decarboxylation of Gly during $H^{13}CHO$ metabolism in YD roots. The great enhancement in the signal peak of [2.3–^{13}C]Su (Fig. 6k) and a huge increment (12-fold) in its yield

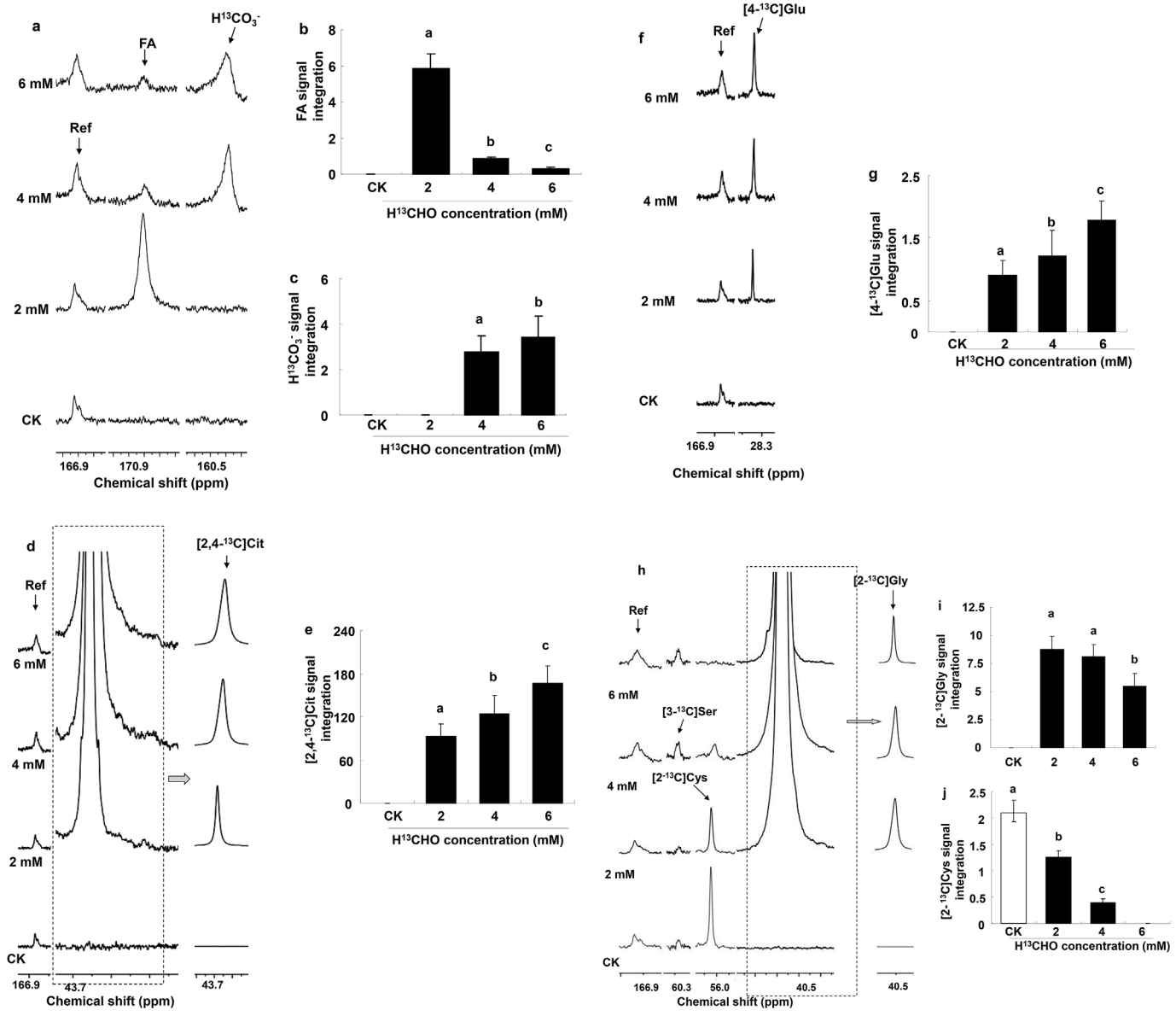

Fig. 3. ^{13}C NMR spectra of YD roots treated with 2, 4 and 6 mM $H^{13}CHO$ for 2 h. The expanded regions of the signal peaks corresponding to $H^{13}CO_3^-$, FA, [2,4–^{13}C]Cit, [4–^{13}C]Glu, [2–^{13}C]Gly, [3–^{13}C]Ser, [U—^{13}C]Gluc and [U—^{13}C]Fruc are shown in (a), (d), (f), (h) and (k). The signal integration of these peaks is shown in (b), (c), (e), (g), (i), (j), (l) and (m).

(Fig. 6m) were observed in CSA-pretreated roots. Accumulation of [2.3–^{13}C]Su was likely the consequence of CSA-inhibited flux of [2.3–^{13}C]Su into the TCA cycle. Taken together, these results indicated that CSA pretreatment did not affect the function of the glyoxylate pathway during $H^{13}CHO$ metabolism in YD roots.

4. Discussion

This study examined the kinetics of HCHO uptake by broad bean roots from HCHO solutions. The HCHO uptake curves in YD roots are similar to those in leaves reported previously (Song et al., 2013; Zhang et al., 2014), displaying a first-slow-later-fast pattern. This dynamics is exactly opposite to the HCHO adsorption kinetics (a first-fast-later-slow pattern) of porous materials (Rengga et al., 2017). The increase in HCHO uptake was small during the 0–2 h period. The greatest increase was observed during the 2–24 h period. The HCHO uptake started to decrease during the 24–48 h period. However, there was no significant difference in HCHO uptake for 2, 4, and 6 mM HCHO solution at each time point. We subtracted the HCHO adsorption by dead roots and HCHO volatilization when calculated the HCHO uptake by living roots. Therefore, the main driving force for HCHO uptake should be attributed to HCHO metabolism in living roots. ^{13}C-NMR analysis showed that the main products of HCHO metabolism in YD roots include FA, CO_2, [2, 4–^{13}C]Cit and [2–^{13}C]Gly. Results from the time-course treatments showed that during the 0–2 h period when these metabolites appeared, the increase in HCHO uptake was slow. During the 2–24 h period when the yield of these metabolites reached their maxima, the greatest increase rate in HCHO uptake was observed. With decreases in signal peaks of these metabolites during the 24–48 h period, the HCHO uptake became small again. According to the relative integration, [2, 4–^{13}C]Cit accounts for ~85% of the total metabolites. Thus, changes in [2, 4–^{13}C]Cit production is closely correlated to HCHO uptake. The ICL activity was induced with the increase in HCHO concentration. As a result, production of [2, 4–^{13}C]Cit also increased in roots, which finally resulted in no significant difference in HCHO uptake of the roots for 2, 4 and 6 mM HCHO.

During seed germination and leaf or fruit senescence, lipids stored in seeds, senescent leaves or fruits are converted to organic acids

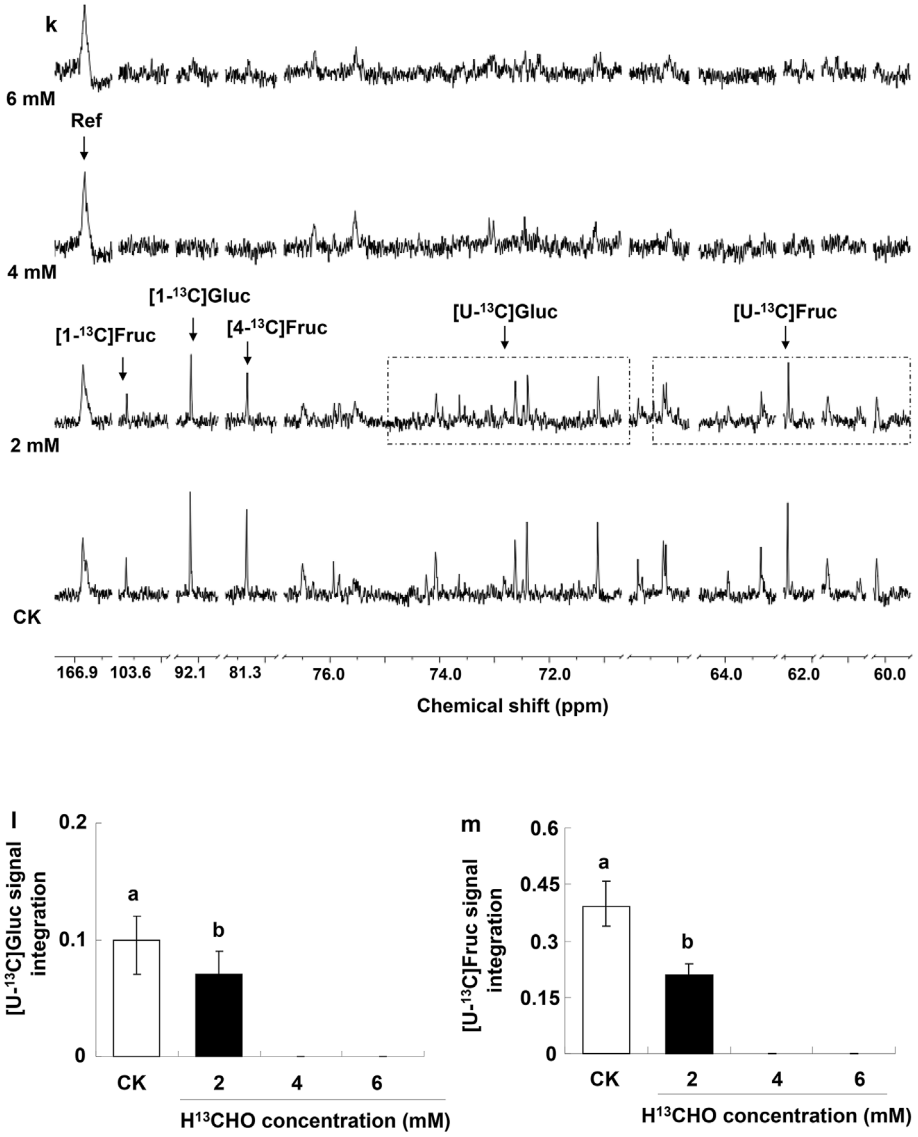

Fig. 3. (*continued*)

through the glyoxylate cycle and the organic acids are then used for sugar synthesis through the gluconeogenesis pathway (Graham et al., 1992; Reynolds and Smith, 1995; Pistelli et al., 1996). Previous studies indicated that sugars inhibit the expression of key enzyme-encoding genes (*ICL* and *MS*) in the glyoxylate pathway in cucumber cultured cells, protoplasts, detached cotyledons, roots or hair roots (Graham et al., 1994; McLaughin and Smith, 1994; Ismail et al., 1997; Sarah et al., 1996). The inhibition is positively correlated with the concentration of endogenous or employed sugars. The evidence indicates that sugars have a feedback inhibition on the function of the glyoxylate pathway in cucumber (Graham et al., 1994; Ismail et al., 1997). Nevertheless, the data of this study indicated that application of glucose, sucrose or mannose at 5–25 mM had no significant inhibition on the ICL activity in YD roots. In contrast, a slight activation of the ICL activity was observed for sucrose and mannose at 5 mM. Thus, sugar inhibition might not be a popular regulation mechanism for the expression of ICL or MS in the glyoxylate cycle in plant roots. Actually, a number of reports have shown that provision of sugars to plant tissues or protoplasts results in either induction or repression of various genes. No production of sugars in $H^{13}CHO$-treated YD roots implied that the glyoxylate pathway did not mediate the conversion of $H^{13}CHO$ to sugar synthesis through the gluconeogenesis pathway. In this context, it is reasonable that the activity of ICL in the glyoxylate pathway in broad bean roots was not be inhibited by sugars.

ICL is a key enzyme of the glyoxylate pathway. The data obtained from enzyme activity analysis showed that the background level of ICL activity in broad bean roots was high. This high background activity enabled a quick function of the glyoxylate pathway in response to HCHO stress in broad bean roots. Moreover, the enzyme activity in YD roots was induced by HCHO. The continuous consume of the absorbed HCHO due to the enhanced HCHO metabolism in roots would cause a decrease in HCHO induction on the ICL activity with the treatment time of 2 mM HCHO increased from 2 h to 12 h and 24 h. As a result, the ICL activity in the YD roots decreased gradually as the treatment time extended from 2 h to 24 h. The elevated concentration of HCHO increased the induction, thus enhanced the ICL activity, and therefore, augmented the role of the glyoxylate pathway in YD roots.

It has been shown that methanol strongly induced the expression of genes involved in HCHO assimilation in methylotrophic yeasts, therefore enhancing the HCHO detoxification. Methanol has a variety of physiological functions in plants, such as promotion of plant growth, regulation of gene and protein expression in plants. Tan et al. (2017) observed that methanol induced the expression of genes related to HCHO metabolism in a black soybean roots. The glyoxylate pathway

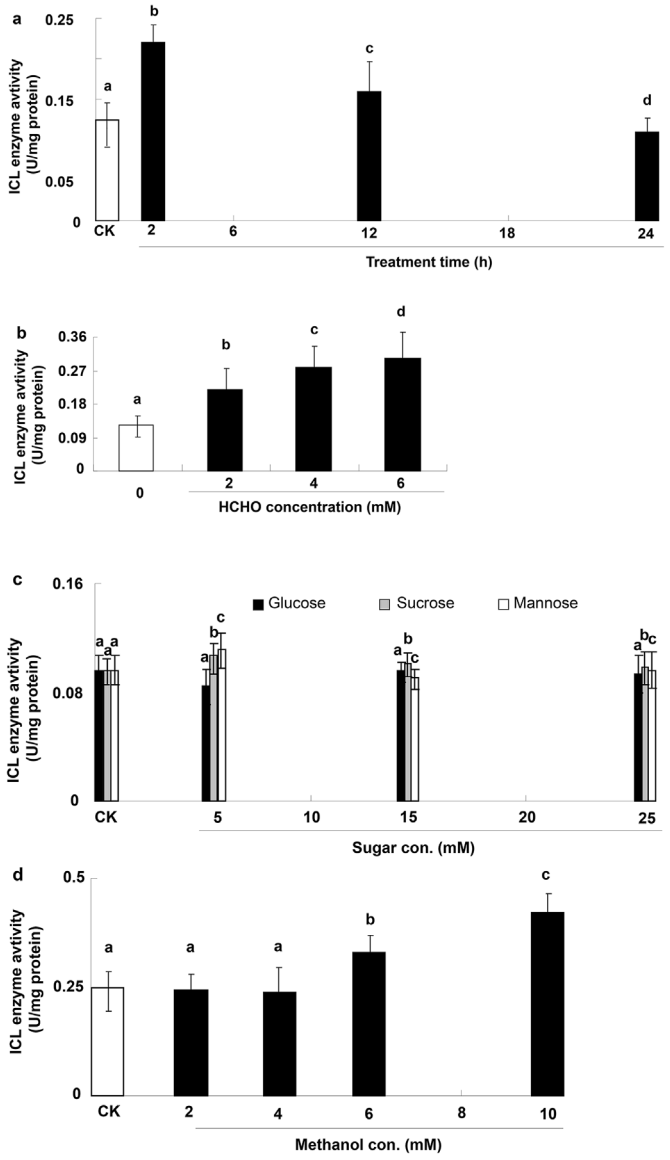

Fig. 4. Effects of sugars, methanol and HCHO on the ICL activity in YD roots. (a) Changes in the ICL activity in YD roots treated with 2 mM $H^{13}CHO$ for 2–24 h. (b) Changes in the ICL activity in YD roots treated with 2 mM–6 mM $H^{13}CHO$ for 2 h. (c) Changes in the ICL activity in YD roots treated with 5–25 mM of glucose, mannose and sucrose for 2 h. (d) Changes in the ICL activity in YD roots treated with 2–10 mM methanol for 2 h.

was the major HCHO metabolic pathway in broad bean roots. The induction of enzymes in the glyoxylate pathway by methanol might be a metabolic response mechanism to HCHO stress that was developed in plants during evolution. This mechanism could play a role when YD roots experienced HCHO stress. In *Aspergillus nidulans*, ethanol can bind with its receptor, a transcription factor, to form a complex which can interact with the cis-acting element in the promoter of ethanol-inducible gene to induce the expression of this gene. We assume that the similar mechanism may also exist in YD roots. There may be cis-acting elements in the ICL gene promoter that can respond to methanol stimulation. Some methanol-bound transcription factors may interact with these cis-acting elements in the ICL promoter to regulate expression of ICL gene, thereby affects ICL activity in YD roots.

Condensation of formate to glyoxylate requires glyoxylate synthase, which is localized in chloroplasts and had been isolated from green potato tubers (Janave et al., 1993). However, this enzyme-encoding gene has not been cloned from any plants to date. There is no sequence information for this gene in broad bean at present and thus, it is difficult to predict the subcellular localization of this enzyme in root cells. According to ^{13}C-NMR data, we speculated that the reaction of formate condensation to glyoxylate should occur during HCHO assimilation in YD roots. However, we did not observe the signal peak of glyoxylate in the ^{13}C-NMR spectrum. Characteristic peaks of glyoxylate were anticipated in ^{13}C-NMR spectra (Supplementary Fig. S5) of green potato tubers treated with $H^{13}CHO$ in a time gradient manner. Contrary to this prediction, no peaks of glyoxylate were observed (Supplementary Fig. S5). However, [2, 4–^{13}C]Cit and [3–^{13}C]Icit (isocitrate) peaks were enhanced (Supplementary Fig. S5), which indicated that the glyoxylate pathway was involved in $H^{13}CHO$ metabolism in green potato tubers. The content of glyoxylate in the metabolic pool in roots of these plant species might be particularly low, which caused the immediate conversion of glyoxylate to other metabolites. The ^{13}C-NMR analysis showed that [3, 6–^{13}C]Cit and [2, 4-C]^{13}Su were metabolites produced from HCHO assimilation through the glyoxylate pathway. The appearance or enhancement in the signal peaks of these two metabolites implied that the glyoxylate pathway played a role during HCHO metabolism. [2, 4–^{13}C]Cit is a representative metabolite of HCHO assimilation via the TCA cycle. CSA is a specific inhibitor of mitochondrial permeability pores and thus, CSA-inhibited generation of [2,4–^{13}C]Cit from HCHO metabolism in broad bean roots is in line with our expectations.

[2–^{13}C]Gly is produced by transamination of glyoxylate, which occurs in peroxisomes (Yu et al., 2010). CSA inhibited the production of [2–^{13}C]Gly. The Peroxisome is an organelle with a special membrane layer. As a result, CSA-inhibited production of [2–^{13}C]Gly might be due to the CSA-hindered the transport of glyoxylate into peroxisomes. The glyoxysome is also an organelle with one layer of membrane. This organelle is not only present in germinating seeds but also in root cells (Shamimuzzaman and Vodkin, 2014). It is puzzled that CSA has no inhibition on [2, 4–^{13}C]Su production in glyoxysome. This evidence suggested that CSA might not inhibit the transport of glyoxylate into glyoxysome because the membrane structure of this organelle is different from that of peroxisomes and mitochondria.

Oxidation of HCHO to formate is almost a common pathway in all plants for HCHO metabolism (Achkor et al., 2003). However, formate is toxic to plants, hence it is often further assimilated into non-toxic metabolites such as sugars, organic acids and amino acids (Kim et al., 2018). Extensive investigations show that there are several entry points for formate into various assimilation pathways. For example, after oxidized to CO_2, formate can be assimilated to sugars through the Calvin cycle, and then may be used to synthesize Gly and Ser via the photorespiration pathway (Song et al., 2013). After entry to the C1 metabolism, formate is first reduced to methylenetetrahydrofolate through a series of folate-dependent reactions and is subsequently assimilated to Ser or Met (Song et al., 2013; Zhang et al., 2014). Formate might be directly condensed to glyoxylate by glyoxylate synthase and afterwards assimilated to organic acids in the glyoxylate pathway (Zeng et al., 2014; Sun et al., 2015; Zhou et al., 2015).

Different from leaf cells, there are no chloroplasts in root cells, thus, HCHO cannot be assimilated through the Calvin cycle in roots. According to ^{13}C-NMR data, the entry point of formate into the assimilation pathway in broad bean roots was likely the condensation to glyoxylate and then entered the glyoxylate pathway. Su produced from the ICL reaction in this pathway shuttled to the TCA cycle and eventually assimilated into [2, 4–^{13}C]Cit. The mechanism of HCHO assimilation in broad bean roots is similar to that observed in geranium leaves (Zhou et al., 2015; Tan et al., 2017). In geranium leaves, HCHO assimilation through the glyoxylate pathway and gluconeogenesis mainly produces [3–^{13}C]Cit and sugars (Zhou et al., 2015; Tan et al., 2017), whereas in broad bean roots the primarily assimilated metabolite was [2, 4–^{13}C]Cit. This is the most important marker metabolite for HCHO assimilation in broad bean roots, which has not been observed in previous studies. Production of a small amount of [2–^{13}C]Gly and

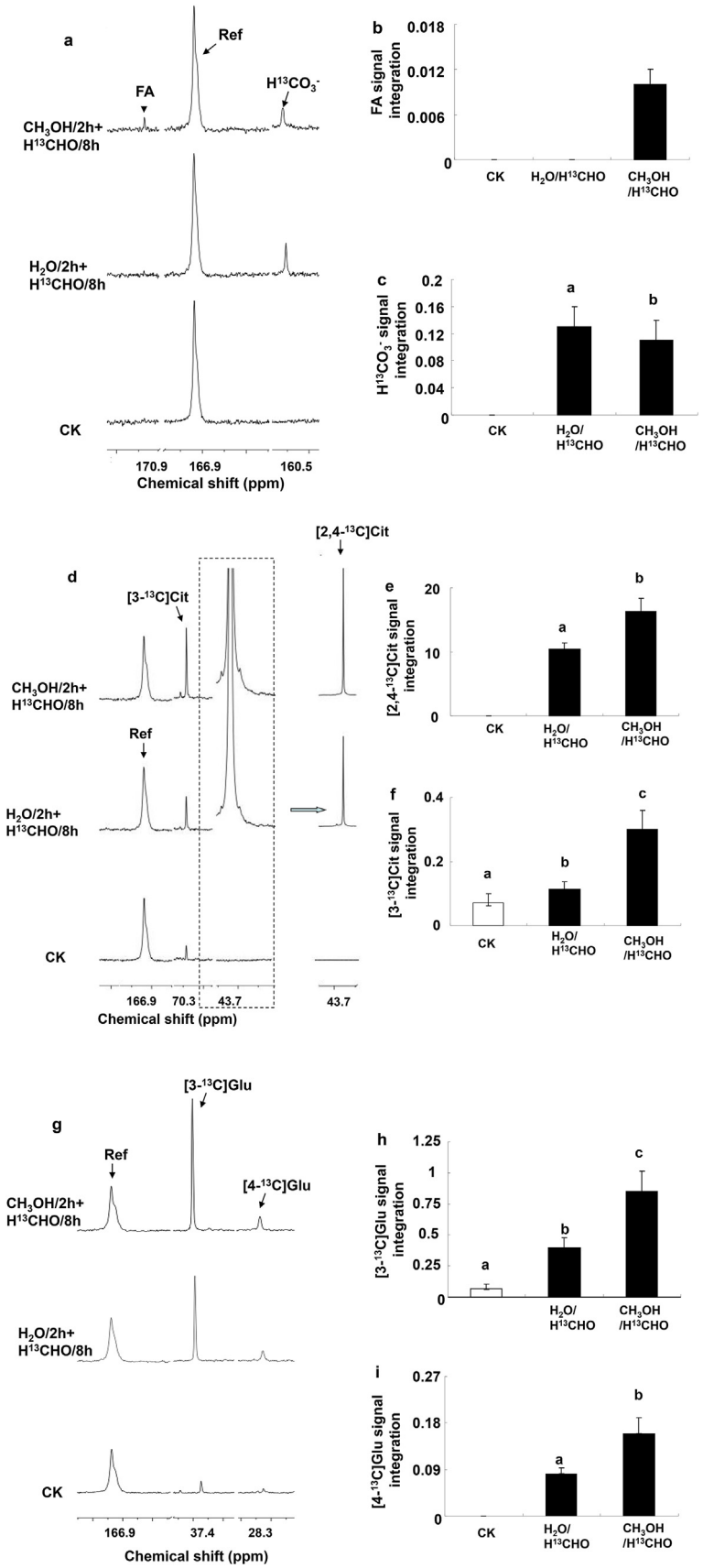

Fig. 5. Comparison of the ^{13}C-NMR spectra of YD roots with ($CH_3OH/H^{13}CHO$) or without ($H_2O/H^{13}CHO$) methanol pretreatment for 2 h followed by 2 mM $H^{13}CHO$ treatment for 8 h. The expanded regions of the signal peaks corresponding to $H^{13}CO_3^-$, FA, 3–^{13}C]Cit, [2,4–^{13}C]Cit, [3–^{13}C]Glu and [4–^{13}C]Glu are shown in (a), (d) and (g). The signal integration of these peaks is shown in (b), (c), (e), (f), (h) and (i).

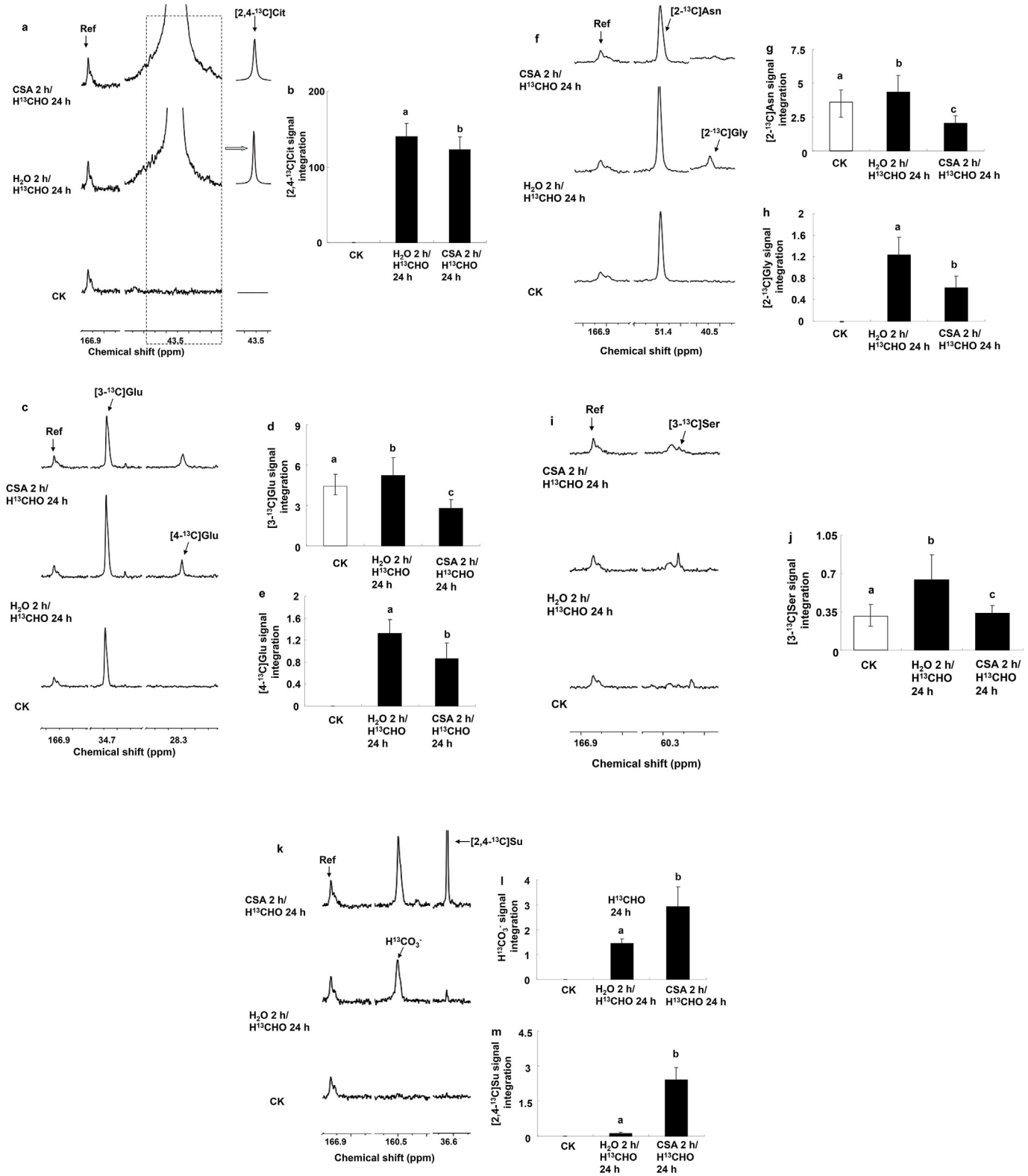

Fig. 6. Comparison of the ^{13}C-NMR spectra of YD roots with (CSA/H^{13}CHO) or without (H_2O/H^{13}CHO) CSA pretreatment followed by 2 mM H^{13}CHO treatment for 24 h. The expanding regions of the signal peaks corresponding to [2,4–^{13}C]Cit, [3–^{13}C]Glu, [4–^{13}C]Glu, [2–^{13}C]Gly, [2–^{13}C]Asn, [3–^{13}C]Ser, [2–^{13}C]Cys, [2,4–^{13}C]Su and H$^{13}CO_3^-$ are shown in (a), (c), (f), (i) and (k). The signal integration of these peaks is shown in (b), (d), (e), (g), (h), (j), (l) and (m).

[3–^{13}C]Ser indicated that the C1 metabolism played a minor role in HCHO metabolism in broad bean roots. In summary, the glyoxylate pathway and TCA cycle played coordinated roles to assimilate the formate, produced from HCHO oxidation, during HCHO metabolism in broad bean roots.

Based on the results obtained from ^{13}C-NMR analysis, a metabolic pathway of HCHO in broad bean roots was proposed (Fig. 7). H^{13}CHO was first oxidized to formate, and most of the formate was then condensed to glyoxylate. A small amount of formate was oxidized to CO_2 (present in the form of HCO_3^-). Glyoxylate entered the glyoxylate

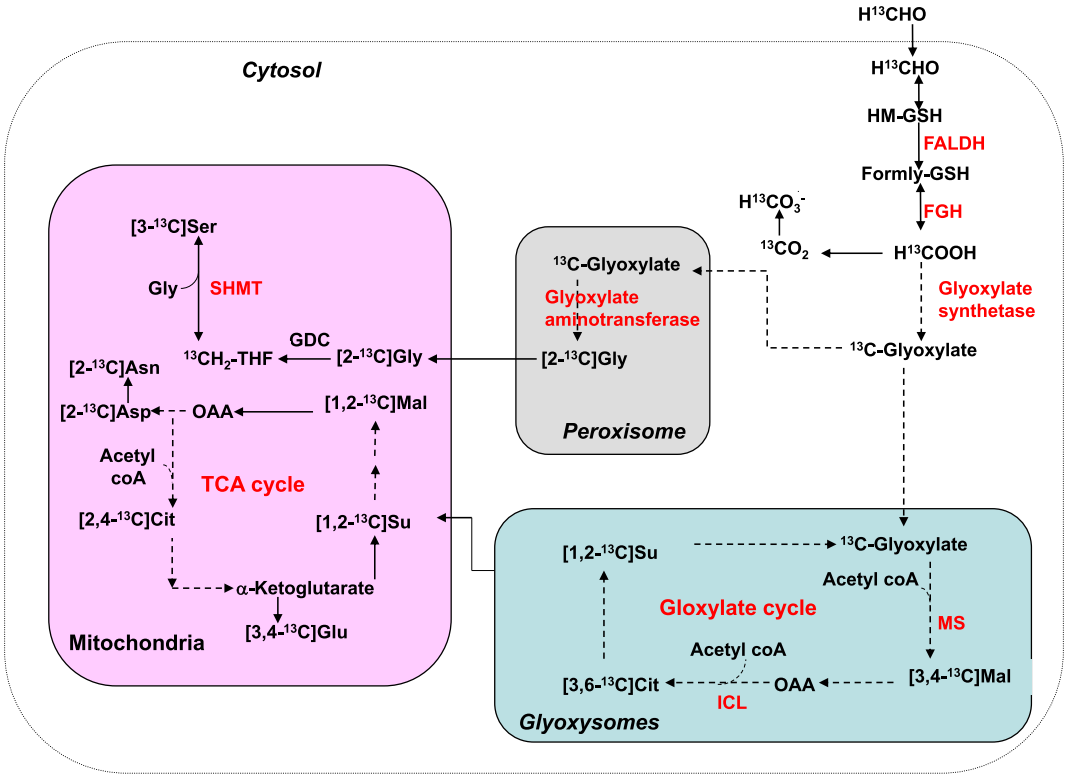

Fig. 7. The diagram of HCHO metabolic pathways in broad bean roots treated with $H^{13}CHO$. The abbreviations are as follows: FALDH, formaldehyde dehydrogenase; HMGSH, S-hydroxymethylglutathione; Formyl-GSH, S-formylglutathione; GDC, glycine decarboxylase; FGH, S-formylglutathionehydrolase; MS, malate synthase; OAA, oxaloacetic acid; ICL, citrate lyase; SHMT, serine hydroxymethyl transferase; Su, succinate; Mal, malate; $^{13}CH_2$-THF, $^{13}CH_2$-tetrahydrofolate.

pathway and was assimilated to [3, 6–^{13}C]Cit and [2–^{13}C]Su. [2–^{13}C]Su shuttled to the TCA cycle and was further assimilated into [2, 4–^{13}C]Cit. The metabolism of [2–^{13}C]Su and [2,4–^{13}C]Cit in the TCA cycle produced OAA and KGA. Subsequent transamination to these metabolites generated [3, 4–^{13}C]Glu, [2–^{13}C]Asp and [2–^{13}C]Asn. A small amount of glyoxylate entered peroxisomes to produce [2–^{13}C]Gly via transamination. Subsequently, metabolism of [2–^{13}C]Gly through the C1 metabolism produced [3–^{13}C]Ser.

5. Author contribution statement

Min processed the data and did most experiments of this paper. Cao performed $H^{13}CHO$ treatment and ^{13}C-NMR analyses for green potato tubers. Xiong and Si prepared broad bean plants and measured the ICL activity for this paper. Dawood Khan did part of writing work and edited the English for this paper. Chen designed experiments and did most writing work for this paper.

6. Compliance with ethical standards

6.1. Conflict of interest

The authors declare no conflict of interest.

Acknowledgments

This work was supported in part by the National Natural Science Foundation of China (Grant # 31560071 to L.M.C.) and by the Foundation of Yunnan Province and Kunming University of Science and Technology for Training Adult and Young Leaders of Science and Technology (Grant # 2004PY01-5 to L.M.C.).

Appendix A. Supplementary data

Supplementary data to this article can be found online at https://doi.org/10.1016/j.plaphy.2019.02.019.

References

Achkor, H., Diaz, M., Fernandez, M.R., Biosca, J.A., Pares, X., Martinez, M.C., 2003. Enhanced formaldehyde detoxification by overexpression of glutathione-dependent formaldehyde dehydrogenase from *Arabidopsis*. Plant Physiol. 132, 2248–2255.
Arora, S., Ramaswamy, N.K., Nair, P.M., 1985. Partial purification and some properties of a latent CO, reductase from green potato tuber chloroplasts. Eur. J. Biochem. 153, 509–514.
Chen, L.M., Yurimoto, H.Li KZ., Orita, I., Akita, M., Kato, N., Sakai, Y., Izui, K., 2010. Assimilation of formaldehyde in transgenic plants due to introduction of the bacterial ribulose monophosphate pathway genes. Biosc. Biotech. Biochem. 74, 627–635.
Chen, Q., Guo, C.L., Wang, P., Chen, X.Q., Wu, K.H., Li, K.Z., Yu, Y.X., Chen, L.M.*, 2013. Up-regulation and interaction of the plasma membrane H^+-ATPase and the 14-3-3 protein are involved in the regulation of citrate exudation from the broad bean (*Vicia faba* L.) under Al stress. Plant Physiol. Biochem. 70, 504–511.
Cooper, T.G., Beevers, H., 1969. Mitochondria and glyoxysomes from castor bean endosperm. J boil Chem 244, 3507–3513.
Feldman, M.Y., 1973. Reactions of nucleic acids and nucleoproteins with formaldehyde. Prog. Nucleic Acid Res. Mol. Biol. 13, 1–49.
Flyvholm, M.A., Andersen, P., 1993. Identification of formaldehyde releasers and occurrence of formaldehyde and formaldehyde releasers in registered chemical products. Am. J. Ind. Med. 24, 533–552.
Graham, I.A., Leaver, C.J., Smith, S.M., 1992. Induction of malate synthase gene expression in senescent and detached organs of cucumber. Plant Cell 4, 349–357.
Graham, L.A., Denby, K.J., Leaver, 1994. Carbon catabolite respression regulate glyoxylate cycle gene expression in cucumber. Plant Cell 6, 761–772.
Ismail, I., Bellis, L.D., Alpi, A., Smith, S.M., 1997. Expression of glyoxylate cycle genes in cucumber roots responds to sugar supply and can be activated by shading or defoliation of the shoot. Plant Mol. Biol. 35, 633–640.
Janave, Machhindra T., Ramaswamy, N. Krishnan, Nair, P. Madhusudanan, 1993. Purification and characterization of glyoxylate synthetase from greening potato-tuber chloroplasts. Eur. J. Biochem 214, 889–896.
Kim, K.J., Khalekuzzaman, M., Suh, J.N., Kim, H.J., Shagol, C., Kim, H.H., Kim, H.J., 2018. Phytoremediation of volatile organic compounds by indoor plants: a review. Horticulture Environment And Biotechnology 59, 143–157.
Lu, Y., Wu, Y.R., Han, B., 2005. Anaerobic induction of isocitrate lyase and malate

synthase in submerged rice seedlings indicates the important metabolic role of the glyoxylate cycle. Acta Biochim. Biophys. Sin. 37, 406–414.
Main, D.M., Hogan, T.J., 1983. Health effects of low-level exposure to formaldehyde. J. Occup. Environ. Med. 25, 896–900.
Maxwell, D.P., Maxwell, M.D., Hanssler, G., Armentrout, V.N., Murray, G.M., Hock, H.C., 1975. Mocrobodies and glyoxylate-cycle enzyme activities in filamentous fungi. Planta 124, 109–123.
McLaughin, J.C., Smith, S.M., 1994. Metabolic regulation of glyoxylatecycle enzyme synthesis in detached cucumber cotyledons and protoplasts. Planta 195, 22–28.
Nash, T., 1953. The colorimetric estimation of formaldehyde by means of the Hantzsch reaction. Biochem. J. 55, 416–421.
Pistelli, L., Nieri, B., Smith, S.M., Alpi, A., De Bellis, L., 1996. Glyoxylate cycle enzyme activities are induced in senescent pumpkin fruits. Plant Sci. 119, 23–29.
Rengga, W.D.P., Chafidz, A., Sudibandriyo, M., Nasikin, M., Abasaeed, A.E., 2017. Silver nano-particles deposited on bamboo-based activated carbon for removal of formaldehyde. Journal of Environmental Chemical Engineering 5, 1657–1665.
Reynolds, S.J., Smith, S.M., 1995. Regulation of expression of the cucumber isocitrate lyase gene in cotyledons upon seed germination and by sucrose. Plant Mol. Biol. 29, 885–896.
Sarah, C.J., Graham, I.A., Reynolds, S.J., Leaver, C.J., Smith, 1996. Distinct cis-acting elements direct the germination and sugar responses of the cucumber malate synthase. Mol. Gen. Genet. 250, 153–161.
Shamimuzzaman, M., Vodkin, L., 2014. Transcription factors and glyoxylate cycle genes prominent in the transition of soybean cotyledons to the first functional leaves of the seedling. Funct. Integr. Genom. 14, 683–696.
Sinha, S.K., Cossins, E.A., 1965. The importance of gyoxylate in amino acid biosynthesis in plants. Biochem. J. 96, 254–261.
Song, Z.B., Xiao, S.Q., You, L., Wang, S.S., Tan, H., Li, K.Z., Chen, L.M., 2013. C1 metabolism and the Calvin Cycle function simultaneously and independently during HCHO-metabolism and detoxification in Arabidopsis thaliana treated with HCHO solutions. Plant Cell Environ. 36, 1490–1506.
Sun, H.Q., Zhang, W., Tang, L.J., Han, S., Wang, X.J., Zhou, S.E., K, K.Z., Chen, L.M., 2015. Investigation of the role of the Calvin Cycle and C1 metabolism during HCHO metabolism in gaseous HCHO-treated petunia under light and dark conditions using 13C-NMR. Phytochem. Anal. 26, 226–235. https://doi.org/10.1002/pca.2556.
Tan, H., Xiong, Y., Li, K.Z., Chen, L.M., 2017. Methanol-enhanced removal and metabolic conversion of formaldehyde by a black soybean from formaldehyde solutions. Environ. Sci. Pollut. Res. 24, 4765–4777.
Wang, R., Zeng, Z.D., Liu, T., Liu, A., ZhaoY, Li, K.Z., Chen, L.M., 2016. A novel formaldehyde metabolic pathway plays an important role during formaldehyde metabolism and detoxification in tobacco leaves under liquid formaldehyde stress. Plant Physiol. Biochem. 105, 233–241.
Xu, Z.J., Cheng, Z.F., Lin, A.J., Wang, J.G., 2008. Removal of formaldehyde from wastewater by activated sludge. Tech. Equip. Environ. Pollut. Control 13, 2–9.
Xu, Z.J., Qin, N., Wang, J.G., Tong, H., 2010. Formaldehyde biofiltration as affected by spider plant. Bioresour. Technol. 101, 6930–6934.
Yu, L., Jiang, J.Z., Zhang, C., Jiang, L.R., Ye, N.H., Lu, Y.S., Yang, G.Y., Liu, W., Changlian Peng, C.L., He, Z.H., Peng, X.X., 2010. Glyoxylate rather than ascorbate is an efficient precursor for oxalate biosynthesis in rice. J. Exp. Bot. 61, 1625–1634.
Zeng, Z., Qi, C., Qi, C., Li, K., Chen, L., 2014. Absorption and metabolism of formaldehyde in solutions by detached banana leaves. J. Biosci. Bioeng 117, 602–612.
Zhang, W., Tang, L.J., Sun, H.Q., Han, S., Wang, X.J., Zhou, S.E., Li, K.Z., Chen, L.M., 2014. C1 metabolism plays an important role during formaldehyde metabolism and detoxification in petunia under liquid HCHO stress. Plant Physiol. Biochem. 83, 327–336.
Zhou, S.E., Xiao, S.Q., Xuan, X.X., Sun, Z., Li, K.Z., Chen, L.M., 2015. Simultaneous functions of the installed DAS/DAK formaldehyde-assimilation pathway and the original formaldehyde metabolic pathways enhance the ability of transgenic geranium to purify gaseous formaldehyde polluted environment. Plant Physiol. Biochem. 89, 53–63.